2014

Feasibility of Automatic Detection of Surface Cracks in Wind Turbine Blades

Huiyi Zhang
Iowa State University, huiyi@iastate.edu

John K. Jackman
Iowa State University, jkj@iastate.edu

Feasibility of Automatic Detection of Surface Cracks in Wind Turbine Blades

Abstract
Cracks on the surface of a wind turbine blade (WTB) can be a sign of current or future damage to the underlying structure depending on the severity of the cracks. We investigated a new method for automatically detecting surface cracks based on image processing techniques. The method was evaluated by varying crack parameters and our method parameters. Identifying and quantifying cracks as small as hair thickness is possible with this technique. Orientation of a crack did not affect the results. The effects of uneven background illumination (present in images captured on-tower) were significantly reduced by optimizing the threshold value for the Canny edge detection method. The accuracy of quantifying a crack was increased by processing an image with both the Sobel and Canny edge detection methods and then combining the results to reduce background noise.

Keywords
gel coat cracks, visual inspection, blades

Disciplines
Industrial Engineering | Systems Engineering

Comments
This article is from *Wind Engineering* 38 (2014): 575, doi: 10.1260/0309-524X.38.6.575. Posted with permission.

Feasibility of Automatic Detection of Surface Cracks in Wind Turbine Blades

Huiyi Zhang and John Jackman
Dept of Industrial and Manufacturing Systems Engineering, Iowa State University, Ames, IA, 50011 U.S.A.

Received 19/06/2013; Revised 09/09/2014; Accepted 14/09/2014

ABSTRACT

Cracks on the surface of a wind turbine blade (WTB) can be a sign of current or future damage to the underlying structure depending on the severity of the cracks. We investigated a new method for automatically detecting surface cracks based on image processing techniques. The method was evaluated by varying crack parameters and our method parameters. Identifying and quantifying cracks as small as hair thickness is possible with this technique. Orientation of a crack did not affect the results. The effects of uneven background illumination (present in images captured on-tower) were significantly reduced by optimizing the threshold value for the ***Canny*** edge detection method. The accuracy of quantifying a crack was increased by processing an image with both the ***Sobel*** and ***Canny*** edge detection methods and then combining the results to reduce background noise.

Keywords: Gel coat cracks, Visual inspection, Blades

1. INTRODUCTION

Visual inspection is widely used as part of routine maintenance programs for large scale structures such as WTBs, aircraft, and bridges. Given the scale of these structures, inspection times are lengthy and the accuracy of the results is highly dependent on the skill of the inspector. Visual inspection is prone to distractions and eye fatigue [1]. For WTB inspection, inspector safety is also a concern because "sky workers" perform the inspection while suspended by a rope attached to the turbine or supported by a platform [2]. An alternative to sky workers is the use of telescopes mounted on the ground. It is well established that eye strain and eye fatigue occur in long term use of telescopes [3]. Visual inspections are not consistent because inspectors vary in their ability to detect small surface flaws (such as hairline cracks) that occur under normal blade operating conditions. Knowing the severity of the crack is important because the potential future damage is proportional to the severity of the crack. Quantifying the location and severity of a crack will enable future technologies that can automate the blade repair process, which is currently a manual labor intensive process.

Accounting for 18% of the total turbine cost, WTBs are a major challenge for maintenance due to the large-scale, on-tower location, and composite materials [4]. The annual Operation & Maintenance (O&M) cost of a wind farm is in the range of 0.5–2.2 cents/kWh depending on turbine size and the useful life of the turbine. O&M costs are 10–20% of the total cost of energy (COE) for a wind project, based on current COE figures of 3.5–6 cents/kWh [5]. Although information is scarce on the cost breakdown of O&M costs, blade failure ranks in the top third of failure rates among all the critical large mechanical components. Blade repair adds a significant downtime per failure, 4 days on average, using expensive cranes and skilled technicians [6]. Early inspection can help prevent severe structural damage and reduce O&M costs (SGS Group, 2010). The SGS Group

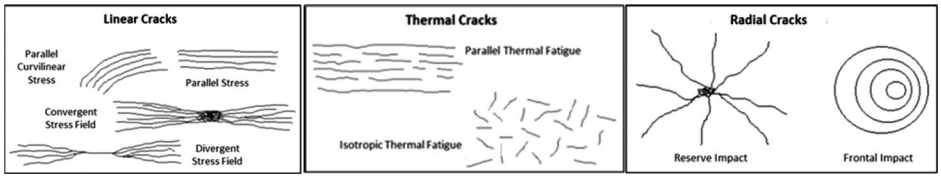

Figure 1. Types of gel coat cracks

points out that repairing a blade (with significant damage) costs 26% of the original blade cost. If the problem is detected early enough by using a third-party inspection company, the cost would be 0.64% of the original blade cost [7].

Turbine blades typically are coated with two thin protective layers, a gel coat and a water-based varnish, to prevent infiltration of moisture, sand, and salt into the underlying fiberglass composite material, which can lead to delamination and other types of structural damage. Depending on the stress applied to a blade surface, gel coat thickness varies between 0.3 mm where loads are light and 0.6 mm along the leading edge where it makes first contact with wind and loads are particularly high [8]. The health of the protective layers is a major O&M concern and is a significant contribution to COE using existing on-tower inspection and repair methods. Companies like BASF have focused their efforts on developing more durable coating materials [9]. However, gel coat defects like cracks and erosion can still occur as early after commissioning a turbine due to environment-related events such as heavy rains. With wind energy moving offshore, the blades will experience a more challenging environment – high moisture and salt – and potentially higher O&M costs.

Cracks that occur in the protective layers include stress cracks, crazing, and thermal cracks as shown in Figure 1. These can significantly reduce the aerodynamic efficiency of blades and lead to structural damage, which is more difficult to detect and repair. This paper addresses the characteristics of the WTB surface cracks and method parameters for automatic computer-aided optical inspection. Similar methods have been studied for aircraft health inspection. For example, a stereoscopic method has been successfully applied to a limited number of surface cracks on aircraft skins [10], [11]. The remainder of the paper is organized as follows. In the next section we describe the methodology of crack detection. Then we present the results for some candidate images, followed by concluding remarks.

2. METHODOLOGY

The three stage crack detection methodology includes: (1) a line detection method to quickly scan a WTB and locate crack regions, (2) an edge detection method that produces a detailed representation of a crack, and (3) a crack quantification method that characterizes the severity of a crack (e.g., size, color) [12]. A series of synthetic cracks were created to control the common characteristics of surface cracks so that we could study the factors that affect the visibility of a crack. Brownian motion was used to create a random crack with correlation between neighboring points on the crack. Variations in thickness and color were also considered.

2.1. Synthetic crack generation

A set of representative synthetic cracks was generated with one-dimensional Brownian motion in a controlled fashion as shown in Figure 2. One-dimensional Brownian motion represents a random displacement from the current location based on a random number generated from a standard normal distribution. The background color of the region surrounding the synthetic cracks was defined as either white or light gray to be consistent with the paint color of a blade. The color of the synthetic crack was varied to represent the severity of a crack. The color of surface cracks gradually changes as the cracks deepen and become easier to identify in digital images. The complexity of a surface crack was reflected in its non-uniform thickness, variation in color, and small deviations along the direction of crack propagation.

Differences in the intensity level of pixels, irregular distribution and geometry of noise (e.g., dirt), and uneven illumination of the image background are three major factors that can decrease the detectability of a crack [13]. The geometry and color of a crack may have some level of impact on the defect detectability. Therefore, we generated three representative groups of synthetic cracks to test the corresponding three hypotheses listed in Table 1.

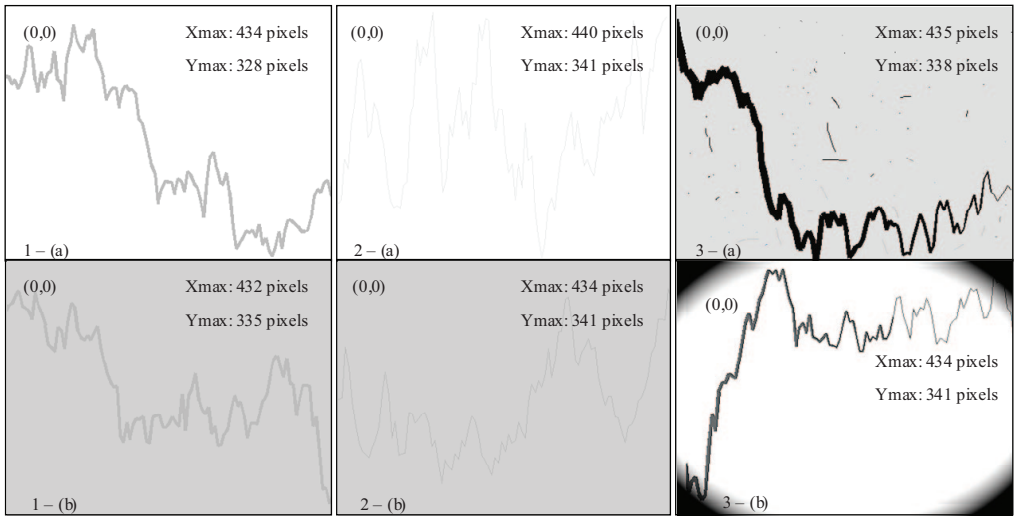

Figure 2. Synthetic cracks: 1. Different intensity level of pixels 2. Hairline thickness cracks 3. Noises & uneven illumination

Table 1. The characteristics of cracks to test the hypotheses

No.	Hypothesis	Characteristics of cracks
1	Different intensity levels of background pixels affect the detectability cracks using image processing techniques.	The color of the cracks is the same, but the background color is either white or light gray.
2	Automatic crack detection can detect small thickness cracks or weak intensity levels of pixels that an inspector would miss.	Small color differences between a crack and its background were used. Crack thickness was set to one pixel.
3	Irregular noise and uneven illumination affect detectability of cracks.	Non-uniform thicknesses of two synthetic crack images were used. One has irregular noise and the other has uneven illumination.

Three field images were selected to further investigate the hypotheses in Table 1 and to evaluate if the parameters that define detectability are consistent with the six synthetic cracks. After testing the method on the three groups of synthetic cracks, the field images shown in Figure 3 were used to evaluate the accuracy of the method. The results were compared to the synthetic cracks to check whether the synthetic cracks captured the basic characteristics of real cracks.

The field images in Figure 3(a) has a hairline crack on the right side and is the most difficult crack to detect with the human eye. Hairline cracks share the same characteristics as the synthetic cracks in the second group as shown in Figure 2-2(a) and (b). Figure 3(b) is a stress crack with uneven background illumination and was used to investigate the effect of the orientation of the line detection masks. The third crack, shown in Figure 3(c), exhibits crazing and significant background noise. Given the spider web geometry, some of the small cracks may not coincide with the four directions of standard line detection masks. The images in Figure 3(b) and (c) were also used to evaluate the effects of uneven illumination and noise on the detectability of cracks, corresponding to the synthetic cracks in group three as shown in Figure 2-3(a) and (b). The background color of Figure 3(a) and (b) was light gray and Figure 3(c) had a white background color, which corresponds to the synthetic cracks in the first group of Table 1.

2.2. Line detection

A line detection method can be used to perform a quick blade scan. It is simple, fast, and sensitive to individual line segments. Cracks can be treated as a set of connected segments. A line is a basic type of intensity discontinuity in a digital image and the most common method to detect them is to

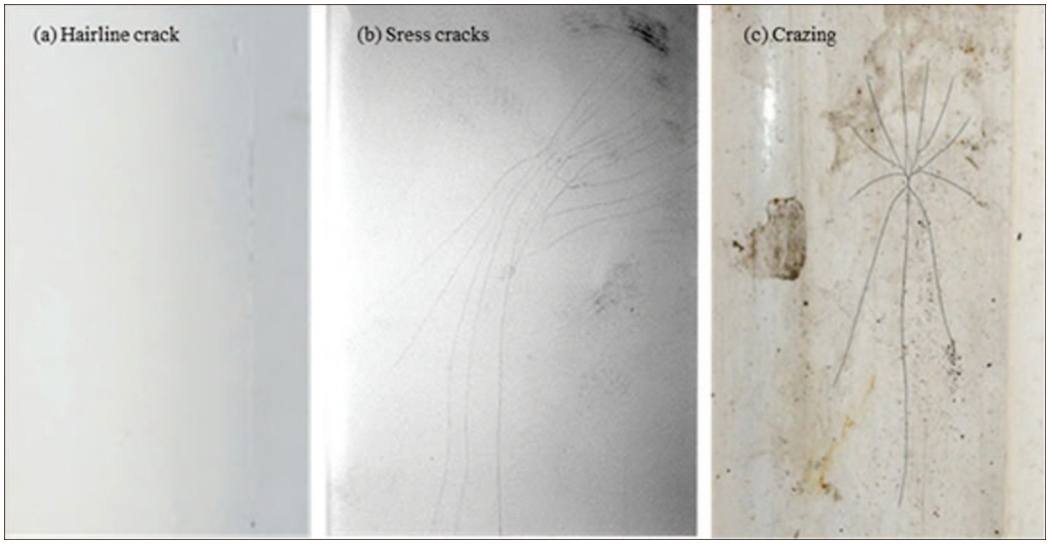

Figure 3. (a) Hairline crack (RGB image: 157-by-272). (b) Stress cracks (Gray-scale: 247-by-350). (c) Crazing (RGB image: 270-by-435)

process the image with a linear spatial filter mask having a binary format. The process consists of moving the center of the mask to each pixel in an image and computing the response at each pixel, which is the sum of the product of the mask coefficients and the intensity of the 8 neighboring pixels and is given by

$$R = \sum_{i=1}^{8} w_i z_i \tag{1}$$

where, z_i is the intensity of the pixel associated with the mask coefficient w_i.

Theoretically, only an odd number size of the mask is considered since R is the response from the center of the filter mask at a specific pixel, (x, y). The smallest mask is a 3 × 3 matrix (i.e., 8 neighboring pixels).There are four standard line detection masks corresponding to the orientation of the lines, namely, horizontal, 45°, vertical, and –45° as shown in Table 2. The larger number – 2 – in the mask matrix represents the direction of the mask and it has a strong response to one pixel thickness segments. Increasing the number from 2 to 3 will smooth the output image but continually increasing the number will create fuzzy results. Although the vertical line detector masks responded strongly to one pixel thickness lines, it can also detect vertical lines with different thicknesses. A binary union operation between the four standard line detector masks creates a composite mask that can detect lines in any direction.

A threshold value was used to convert a gray-scale image to a binary image. Suppose $f(x, y)$ represents the intensity of a pixel at (x, y) and T is a selected threshold value, any pixel where $f(x, y) \geq T$ is set to 1 and is classified as an object pixel. Otherwise, the pixel is set to 0 and is classified asa background pixel. The converted image $g(x, y)$ is defined as

$$g(x,y) = \begin{cases} 1 \; if \; f(x,y) \geq T \\ 0 \; if \; f(x,y) < T. \end{cases} \tag{2}$$

The MATLAB toolbox provides a function, *graythresh*, that computes a threshold using Ostu's method [13]. However, this method tends to generate significant noise when the background illumination is uneven.

Table 2. Standard line detector masks

–1	–1	–1
2	2	2
–1	–1	–1

(a) Horizontal.

2	–1	–1
–1	2	–1
–1	–1	2

(b) 45°.

–1	2	–1
–1	2	–1
–1	2	–1

(c) Vertical.

–1	–1	2
–1	2	–1
2	–1	–1

(d) –45°.

2.3. Edge detection

A major advantage of edge detection is that uneven illumination does not affect the detectability of an edge. Edge detection was used to capture the outer contour of non-uniform thickness cracks and to complement the inadequacy of line detectors in detecting meaningful discontinuities in intensity values. Unlike line detection, edge detection uses first- or second-order derivatives to compute the maximum rate of change of grayscale levels of pixels. Edge detection gave much smoother results by eliminating noise having a small number of pixels. However, this process may take a long time when the size of the images are large (e.g., 2 MB). Therefore, line detection was applied first so that a fast scan of the entire blade can be performed in a reasonable amount of time and then the edge detection method was used to extract detailed information from the areas identified by line detection.

The MATLAB function, *edge* (), supports several common detection methods including: *Sobel*, *Prewitt*, *Laplacian* of a Gaussian (LoG), and *Canny*. The key difference between these methods is how the first or second-order derivatives are approximated. The first order derivative in image processing is a vector for a 2D function $f(x, y)$ given by

$$\nabla f = \begin{bmatrix} G_x \\ G_y \end{bmatrix} = \begin{bmatrix} \frac{\partial f}{\partial x} \\ \frac{\partial f}{\partial y} \end{bmatrix} \tag{3}$$

with the magnitude of the vector being $g = mag(\nabla f) = \left[G_x^2 + G_y^2 \right]^{1/2}$ and the angle is $\alpha(x,y) = \tan^{-1}\left(\frac{G_x}{G_y}\right)$ defines the edge direction. Both the *Sobel* and *Canny* methods were considered since *Sobel* is the most commonly used and *Canny* is considered to be the most powerful edge detector. The *Sobel* method had default masks as shown in Table 3 to compute the gradient, ∇f, which is composed of vectors G_x and G_y, given by

$$\begin{aligned} G_x &= (z_7 + 2z_8 + z_9) - (z_1 + 2z_2 + z_3) \text{ and} \\ G_y &= (z_3 + 2z_6 + z_9) - (z_1 + 2z_4 + z_7). \end{aligned} \tag{4}$$

where z_1, ... z_9 are the pixel values of the pixel neighborhood and pixel z_5 is the pixel that the mask is being applied to as shown in Table 4.

The *Canny* method is more complex and includes a Gaussian filter, a local gradient, an edge direction computation algorithm, and provides edge linking by incorporating the weak pixels that are connected to the strong pixels.

The default threshold number for the *Sobel* and *Canny* methods does not guarantee a accurate result. However, both of these methods offer promising results by optimizing the threshold value. The *Sobel* method offered less noisy results as compared to the *Canny* method but also tended to miss a significant number of the defects. By updating the threshold number, the *Canny* method produced the smoothest result. The *Sobel* method did not reduce the background noise significantlyas the threshold value was adjusted. On the other side, the noise generated by *Sobel* method looks like points, where the *Canny* method produced noise that tended to be small segments. If we treat the noisy results as connected pixels, then we can filter them by eliminating number of

Table 3. *Sobel* detector masks

−1	−2	−1
0	0	0
1	2	1

(a) Vertical.

−1	0	1
−2	0	2
−1	0	1

(b) Horizontal.

Table 4. *Pixel Neighborhood*

z_1	z_4	z_7
z_2	z_5	z_8
z_3	z_6	z_9

connected pixels less than a specific threshold value, say 3 pixels. With this method, *Sobel* method can eliminate noisy results better since the noisy results generated by *Sobel* method are small dots.

Adjustment of the edge detection threshold values requires a lot of human intervention, which is not the goal of this research. The default threshold value was used as a starting point and was adjusted using a fixed step size. The edge detection method was performed with the new threshold value and the results were compared with the previous results to determine if the difference is within an acceptable tolerance. For example, the default threshold value for the *Canny* method is $T = [t_1, t_2]$ that produces an image A_0 containing all the detected edges corresponding to the cracks. The threshold value was updated to $T_1 = [t_1 + .1 \times (t_2 - t_1), t_2 - .1 \times (t_2 - t_1)]$ and applied again, producing a new set of detected edges in image A_1. The process was repeated until $A_{i+1} - A_i \geq D$, where D is standard deviation of all As.

2.4. Quantifying crack severity

Two methods were used to quantify the severity of a crack. The easiest method was to find the bounding rectangle (parallel to the x and y axes) that encloses the pixels from the edge detection method. This region identified the most likely required repair area. However, it did not provide any further information about the orientation of the crack and tended to overestimate the magnitude.

The second approach was to find the minimum enclosing envelope (i.e., the envelope orientation is not constrained). The envelope can be found by estimating the parameters of a line that minimizes the maximum distance to all the points on the crack edges. Using the start and end points of the detected edges, the sides of the envelope can be found by projecting the end points onto the estimated line. The other two sides of the envelope correspond to the maximum deviation of the crack on each side of the line.

To minimize the maximum distance to the line, the function *fminimax* in MATLAB was used to find the best fit parametric line, denoted by $\begin{cases} x=at+b \\ y=ct+d \end{cases}$. The function, *fminimax*, requires an initial guess for the parameters of the line [a, b, c, d] and a function that computes the maximum distance of all points along the edges to the given line. The function stops when the change in [a, b, c, d] values is within a specified tolerance (i.e., the change is negligible) or a maximum number of iterations is reached. The default iteration limit is 500 in MATLAB. In this study a limit of 2500 iterations was used.

2.5. Potential errors

Any inspection technique can result in two kinds of errors: false-positive (Type 1) or a defect is missed (Type 2). For crack detection, a Type 1 error can be caused by noise, which cannot be totally avoided. Missing a defect (Type 2) could occur due to uneven illumination or line and edge detection method parameters. The consequences of a Type 1 error in this context are not as severe as the Type 2 error, since missing defects can lead to ignoring the necessary maintenance, leading to future structural damage. Type 2 error can be reduced significantly by adjusting the threshold values.

3. RESULTS

The results of the image processing show that (1) noise, intensity level of pixels, and uneven illumination are major factors that affect detectability, (2) the line detection method is capable of quickly scanning a blade to find crack regions, and (3) uneven illumination is not a major factor in edge detection methods. The *Canny* method offers the best results in detecting discontinuities in the surface. The severity of a crack is difficult to quantify because we only considered 2D images in the paper. However, the crack size and intensity level of pixels offer important insights on the magnitude of a crack.

The six synthetic cracks and three representative field images were tested with both line and edge detection methods. The *Canny* method had the best results by far in terms of detecting discontinuities in the surface. Generally, uneven illumination had much less influence on the detectability of edge detection methods as compared to line detection. For a very bright background, edge detection offered much better results. Unlike line detection, edge detection eliminated low levels of noise and the detected edges were much smoother.

3.1. Factors affecting detectability

The intensity level of pixels is important. The results for the first group of synthetic cracks showed that our method can detect a crack regardless of background color. When applying the MATLAB

graythresh function, the two images resulted in very different optimal threshold numbers and clearly delineated defects. Not surprisingly, the applicable threshold range was significantly different for the two images. The image with a white background had lower and upper threshold values of 0.746 and 0.999, respectively. The image with a gray background had lower and upper threshold values of 0.745 and 0.827, respectively. Upper threshold values eliminated more noise with low- to middle-level intensity levels for pixels in the background, which can make the results more definitive if there is a lot of noise in the background. However, the tradeoff is that some of the defects will be filtered out if the defect has a lower intensity level than the noise in the background.

Surprisingly, crack thickness did not affect the detectability of a crack for synthetic cracks and field images. Also, crack orientation was not a significant factor. In the line detection method, when images were rotated counter-clockwise in 10 degree increments, the line detector masks were able to detect lines in all orientations. Edge detection methods are based on first- or second- order derivatives, which are not affected by crack orientation. Therefore, both line and edge detection methods were not affected by crack orientation. In other words, the orientation of the field camera is not expected to affect the results.These results suggest that the computer-based method is amenable to on-tower inspection of blades that would be in different orientations.

Background illumination is important because automatic threshold computing methods tend to fail when the background illumination of an image is uneven (i.e., there is variance in the pixel values). Uneven illumination had a major effect on the line detection method as shown in Figure 4(b). The original image of stress cracks in Figure 3(b) had very bright lighting on the background and the results were poor. Therefore, the lighting problem still poses a challenge for line detection. This problem can be addressed to a limited extent with existing image processing techniques. Further research is warranted to reduce the effects of uneven lighting on crack detection. Edge detection methods reduce the uneven illumination problem for the same cracks as shown in Figure 5(b) and (d). Also edge detection methods reduce the background noise problem for the crazing cracks shown in Figure 6. This supports the hypothesis we made earlier that it would be most effective to use the line detection method to perform a quick scan and then apply an edge detection method to investigate the details of a crack.

3.2. Edge detection

Edge detection methods like *Sobel* and *Canny* produced much smoother results than the line detection method. Noise and uneven illumination did not have a significant impact on edge detection. The intensity level of pixels is very important to both line and edge detection methods

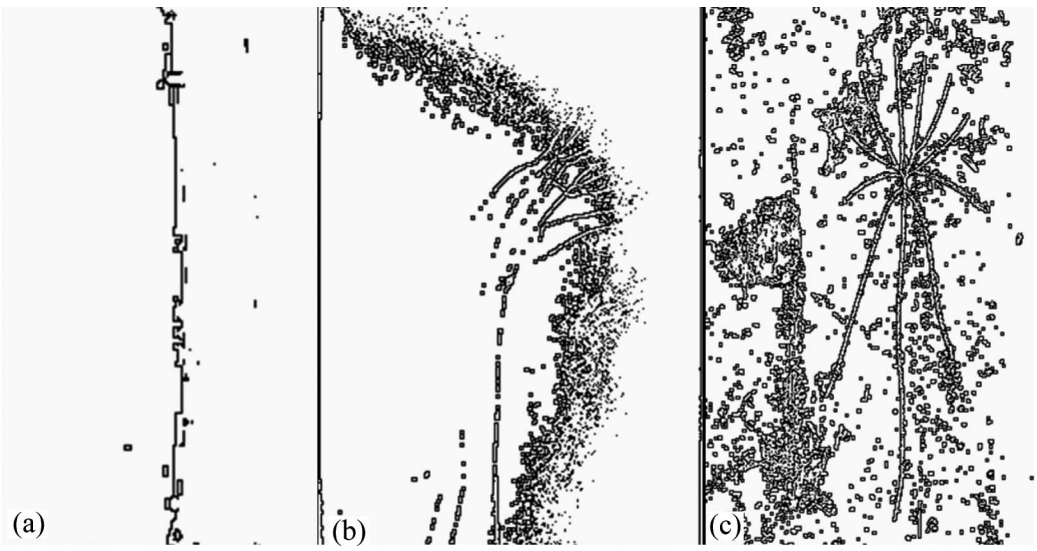

Figure 4. Field images after line detection (a) Hairline crack (b) Sress cracks (c) Crazing

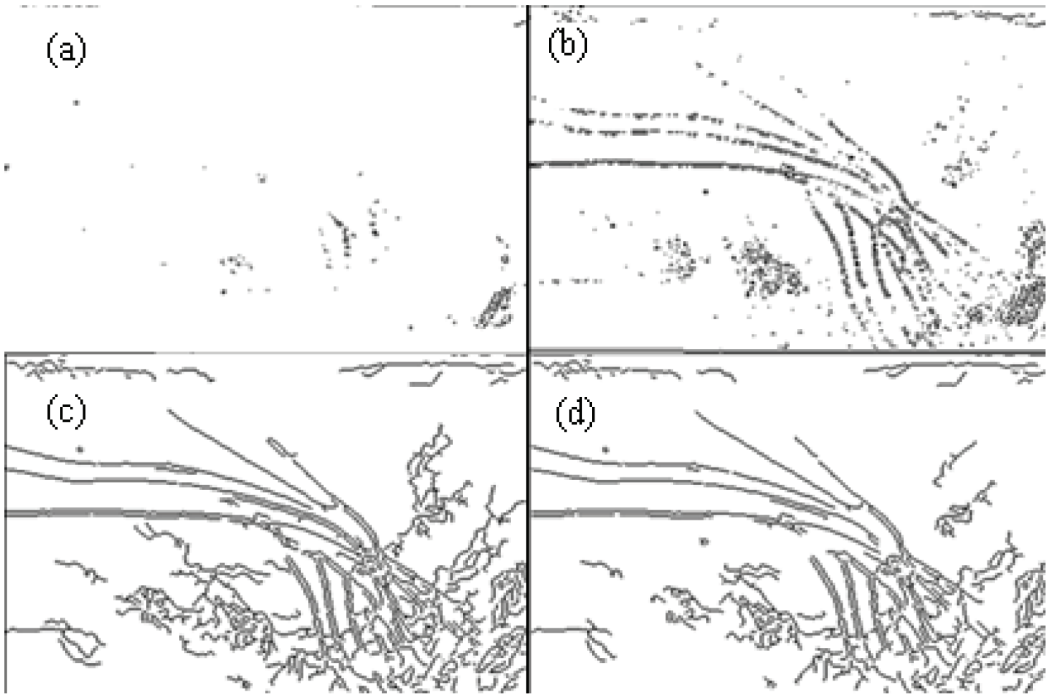

Figure 5. Edge detection with different threshold values. (a) ***Sobel*** method with default threshold (b) ***Sobel*** method with optimal threshold (c) ***Canny*** method with default threshold (d) ***Canny*** method with optimal threshold

because if the intensity level of noise is larger than the intensity level of the defect, the defect will not be detected since the method will consider it to be background noise and eliminate it.

When testing synthetic cracks with the line and edge detection methods, the first two groups of synthetic cracks had the same results. Neither the color or size of the crack affected the result. In other words, both the line and edge detection methods could easily detect hairline cracks when there is no significant background noise or no uneven illuminations. However, both the *Sobel* and *Canny* methods required adjustments to the threshold values to detect some cracks. Without these adjustments, these methods had difficulty detecting stress cracks under uneven illumination conditions and crazing cracks with noisy backgrounds.

With the default threshold value, *Canny* method offered much better results as shown in Figure 5(c), where *Sobel* method missed a significant number of cracks as shown in Figure 5(a). Both the *Sobel* and *Canny* methods could produce better results by optimizing the threshold values as shown in Figure 5(b) and (d). The *Canny* method result is much smoother but also noisier as shown in Figure 5(d).

The crazing crack from Figure 3(c) contains a lot of noise, which is common to blades. Both the *Canny* and *Sobel* methods were able to reduce the background noise effect, which means the computer-based optical inspection method is feasible for on-tower inspection (see Figure 6).

3.3. Quantifying the cracks

After the cracks were detected, they were bounded in a rectangle and a minimum enclosing envelope. The rectangle indicated the recommended repair area. The envelope provided additional information on the direction and magnitude of the cracks. However, if there was a lot of noise, the parallel lines were just the lines enclosing all the noise such as in in Figure 4(c). Therefore, eliminating noise as much as possible is very important in estimating the magnitude of a crack.

The first synthetic crack in Group 1 was selected to demonstrate the capability of quantifying a crack since the direction of the crack is clear and it is easy to determine if the approximation line follows the direction of the crack. First, the recommended repair area is enclosed in the yellow rectangle with 423-by-301 pixels as shown in Figure 7, where the original image has 434-by-328

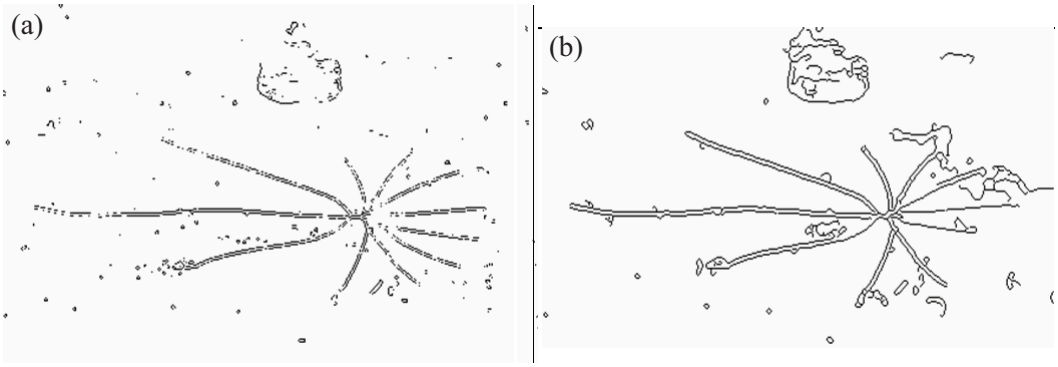

Figure 6. Edge detection reduce noise significantly (a) ***Sobel*** method (b) ***Canny*** method

pixels shown in Figure 2-1(a). The minimum envelope for the crack was bounded by the light blue lines that are parallel to the purple line with parametric equations listed below.

$$\begin{cases} x = 439.2590 * t + 202.6571 \\ y = 277.2023 * t + 166.7593 \end{cases} \quad (5)$$

where $t \in [-0.46, 0.502]$.

The two parallel lines in light blue enclosed the cracks with minimum distance to the purple line as shown in Figure 7. The severity of a crack was defined by its intensity along the crack. The location of the cracks on the blade can be critical. For instance, if a crack occurred along the leading edge or the root section, it may create greater damage or accelerate structural damage than in other areas since the leading edge contacts the wind first and the root section is affected by a greater accumulation of fatigue loads.

3.4. Example from field images

A set of 27 field images were collected by Fraunhofer-IWES at a nearby wind farm in August 2011. The 27 images were processed with the edge detection methods and the results were consistent. One of the sample cracks that was detected and quantifiedis shown in Figure 8.

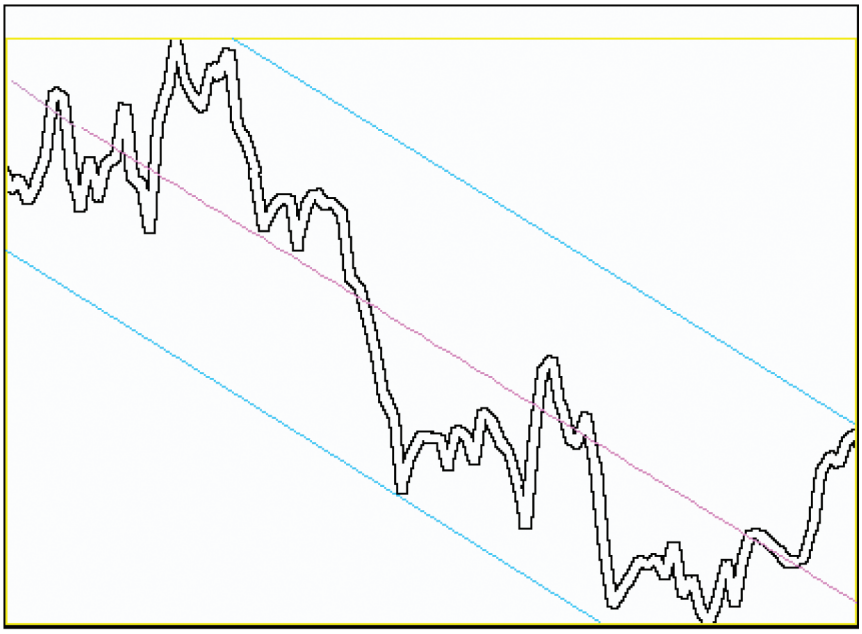

Figure 7. Quantification of the synthetic crack in Figure 2-1-(a)

(a) Field image with faint crack (magnified 3X)

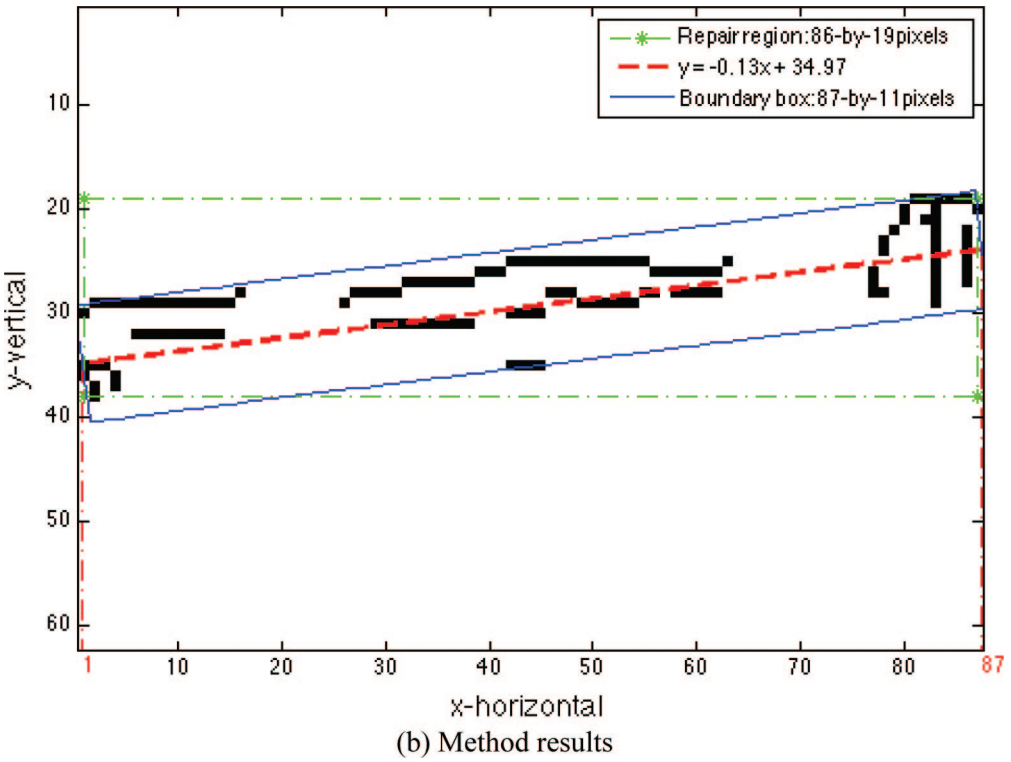

(b) Method results

Figure 8. Quantification of a field image with a crack

4. CONCLUSION AND FUTURE WORK

This paper evaluated image processing techniques for detecting cracks in wind turbine blades, namely, the line detection method and the *Sobel* and *Canny* edge detection methods. Uneven illumination and background noise in blade images had the most impact on the quality of the results. Threshold values for the methods are critical for the successful detection of cracks. We have described an iterative method that automatically finds a suitable threshold value. Given the negligible computation time required by the line detection method, it is ideally suited for quick scans of the entire blade surface. It can quickly identify hairline cracks that are invisible to the naked eye. Image processing thresholds and filters can be used to minimize false-positives caused by surface irregularities like dirt or dust. However, this approach does not work well for obtaining detailed information about a crack because of the effect of uneven illumination.

Edge detection methods provide more detailed information about cracks than line detection, but these methods have difficulty distinguishing between surface irregularities and cracks. A two stage analysis is recommended. First, identify crack regions using the line detection method, reducing the amount of subsequent image processing to only those areas where cracks have been detected. Then

the list of crack regions is analyzed with edge detection to produce more information about the cracks. Edge detection is particularly useful when there is uneven illumination.

The results showed that automated optical inspection for crack detection shows promise for maintenance work on in-service wind turbine blades. With a high quality image and processing tools, image processing techniques can consistently identify cracks that are invisible to human eyes, even when looking at the blade from different angles. Further research is necessary to apply these methods to more sample cracks and to investigate methods that minimize errors caused by uneven lighting and noise.

ACKNOWLEDGMENT

I would like to thank my major professor, Dr. John Jackman, for all of his support and masterful editing assistance, and my host Benjamin Buchholz and Florian Sayer, for all of their support while I was staying at the Fraunhofer IWES. The work reported in this paper was supported [in part] by the U.S. National Science Foundation through its Integrated Graduate Education and Research Traineeship (IGERT) Program, award 1069283.

REFERENCES

[1] Trimm, M. An overview of nondestructive evaluation methods. Practical Failure Analysis 3.3 (2003): 17–31.

[2] Marsh, G. Meeting the challenge of wind turbine blade repair. Reinforced Plastics, July–August, 2011, Vol. 55(4), p. 32(5).

[3] Hanson, R. J. E. Visual fatigue and eye strain in the use of telescopes. Transactions of the Optical Society 22.1 (1920): 26.

[4] Hutchinson, J.R., Schubel, P.J., and Warrior, N.A., A cost and performance comparison of LRTM and VI for the manufacture of large scale wind turbine blades, Renewable Energy, 36 (2011) pp. 866–871.

[5] Walford, Christopher A. Wind turbine reliability: Understanding and minimizing wind turbine operation and maintenance costs, Global Energy Concepts, LLC. Sandia Report: SAND2006-1100 Mar. 2006.

[6] Hahn, B. (1999). "Reliability Assessment of Wind Turbines in Germany." 1999 European Wind Energy Conference, Nice, France, March 1–5.

[7] SGS Group, The cost of wind blade inspections versus blade repair. Hamburg, Germany, available on-line at http://www.nacleanenergy.com/oldsite/index.php?option=com_content&view=article&id=2327:the-cost-of-wind-blade-inspections-versus-blade-repair&catid=42:feature-articles&Itemid=109.

[8] ABB robotics. "ABB Robotics – Painting wind turbine rotor blades." Dec., 2009, available on-line at http://robotize.com.au/roboticnews/videos/25ba98/ABB-Robotics-Painting-wind-turbine-rotor-blades/.

[9] BASF, "Chemistry makes wind power more economic.", "New epoxy resin for high-performance rotor blades.", and "Special protective coating increases the profitability of wind turbine systems." Aug. 2014, Available on-line at http://www.basf.com/group/corporate/en/sustainability/environment/climate-protection/solutions/energy

[10] Siegel, M., Enhanced remote visual inspection of aircraft skin. Robot Institute. Carnegie Mellon University. Proceedings of the Intelligent NDE Sciences for Aging and Futuristic Aircraft Workshop, September, 1997, pp. 101–112.

[11] Alberts, C. J., Carroll, C. W., Kaufman, W. M., Perlee, C. J., and Siegel, M. W. (1998). Automated Inspection of Aircraft (No. AAR-430). Carnegie Mellon Institute of Research, Pittsburgh, PA.

[12] Zhang, H. and Jackman, J. A feasibility study of wind turbine blade surface crack detection using an optical inspection method, Renewable Energy Research and Applications (ICRERA), 2013 International Conference on, published in 2013, pp. 847–852, DOI: 10.1109/ICRERA.2013.6749869.

[13] Gonzalez, Rafael C. Digital Image Using MATLAB Processing. Upper Saddle River, New Jersey, 2004, Pearson Education, Inc.